

Energy Technology

Generation, Conversion, Storage, Distribution

3/2014



Cover Picture: Power generation using thermoelectric windows for green building technology
(S. B. Inayat and M. M. Hussain)

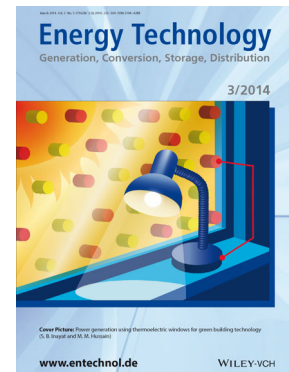
www.entechinol.de

WILEY-VCH

Cover Picture

Salman B. Inayat*, Kelly R. Rader, and Muhammad M. Hussain*

Thermoelectric windows: A thermoelectric generator is embedded into a window glass that can generate 300 Watts of power at a temperature difference of 20 °C, achieving a new breakthrough in green building technology, as described in the Full Paper by Prof. Muhammad M. Hussain and colleagues at the King Abdullah University of Science and Technology on page 292. Forty percent of global energy consumption is related to room heating and cooling. Therefore, thermoelectric generators integrated into building materials can generate thermoelectricity based upon the temperature difference between the outside temperature and inside building temperature. One major challenge is to have a thermopile that is thick enough (at the least 5 mm in alignment with standard glass thickness). The micrometer-sized thermoelectric powders were therefore ball milled into nanostructured materials and then hot pressed into a mold to form 5 mm thermopiles before inserting into the window glass to make thermoelectric windows.



E-Mail Address

[Forgotten Password?](#)

Log In

[Register](#)[Institutional Login](#) Remember Me

ULLMANN'S ENCYCLOPEDIA OF INDUSTRIAL CHEMISTRY
Built from generations of expertise, for generations to come.

Find news, sample content and more ▶▶▶

WILEY-VCH

Home > Chemical Engineering > General & Introductory Chemical Engineering > Energy Technology

JOURNAL TOOLS

- Get New Content Alerts
- Get RSS feed
- Save to My Profile
- Get Sample Copy
- Recommend to Your Librarian

JOURNAL MENU

[Journal Home](#)

FIND ISSUES

[Current Issue](#)
[All Issues](#)

FIND ARTICLES

[Early View](#)
[Most Accessed](#)
[Most Cited](#)

GET ACCESS

[Subscribe / Renew](#)

FOR CONTRIBUTORS

[Author Guidelines](#)
[For Referees](#)
[OnlineOpen](#)
[Submit an Article](#)

ABOUT THIS JOURNAL

[Contact](#)
[Editorial Board](#)
[Advertise](#)
[Overview](#)

SPECIAL FEATURES

[Cover Gallery](#)
[Read Cover Story](#)

Energy Technology

Generation, Conversion, Storage, Distribution

Energy Technology

© WILEY-VCH Verlag GmbH & Co. KGaA, Weinheim



Impact Factor: 2.824

ISI Journal Citation Reports © Ranking: 2014: 31/89 (Energy & Fuels)

Online ISSN: 2194-4296

Associated Title(s): [Advanced Energy Materials](#), [Chemical Engineering & Technology](#), [Chemie Ingenieur Technik](#), [ChemSusChem](#)

Recently Published Issues | [See all](#)

Current Issue: October 2015

Volume 3, Issue 10

September 2015

Volume 3, Issue 9

August 2015

Volume 3, Issue 8

July 2015

Volume 3, Issue 7

June 2015

Volume 3, Issue 6

New Journal | [Recommend to Library](#)

Energy Technology publishes articles covering all technical aspects of energy process engineering from different angles, e.g.,

- new concepts of energy generation and conversion
- design, operation, control, and optimization of processes for energy generation (e.g., carbon capture) and conversion of energy carriers
- improvement of existing processes
- combination of single components to systems for energy generation
- design of systems for energy storage
- production processes of fuels, e. g., hydrogen, electricity, petroleum, biobased fuels
- concepts and design of devices for energy distribution

[Recommend to your librarian](#)

E-alerts for new articles | [Sign up now](#)

News

Energy Technology is fully listed in the ISI/Web of Knowledge (WoK) database and Science Citation Index (SCI) from Thomson Reuters, and its inaugural impact factor was announced to be 2.824. Thank you for your support! You can follow Energy Technology on Twitter at [@EnergyTechnol](#).

Call for Papers | [Why you should submit](#)

- Online submission
- Fast and rigorous peer-review process
- Electronic proofing
- EarlyView for rapid online publication
- Open Access publishing option
- Fast high quality publication
- Supporting Information
- Thomson Reuters (ISI) citation tracking
- Included in all major bibliographic databases
- High visibility and international readership
- Notification of published research
- Comprehensive social media coverage

SEARCH

In this journal

[Advanced >](#) [Saved Searches >](#)

SEARCH BY CITATION

Volume: Issue: Page:



**Maximize
the impact
of your
published
research**

**Free author
promotional toolkit**



Wiley Online Library

Publications

[About Us](#)

Browse by Subject

[Help](#)

[Contact Us](#)

Resources

[Agents](#)

[Advertisers](#)

[Media](#)

[Privacy](#)

[Cookies](#)

[Terms & Conditions](#)

[Site Map](#)

Copyright © 1999-2015 John Wiley & Sons, Inc. All Rights Reserved.

[About Wiley](#) [Wiley.com](#) [Wiley Job Network](#)






WILEY

Wiley
presents...

WILEY

[Home](#) > [Chemical Engineering](#) > [General & Introductory Chemical Engineering](#) > [Energy Technology](#)

JOURNAL TOOLS

-  [Get New Content Alerts](#)
-  [Get RSS feed](#)
-  [Save to My Profile](#)
-  [Get Sample Copy](#)
-  [Recommend to Your Librarian](#)

JOURNAL MENU

[Journal Home](#)

FIND ISSUES

[Current Issue](#)
[All Issues](#)

FIND ARTICLES

[Early View](#)
[Most Accessed](#)
[Most Cited](#)

GET ACCESS

[Subscribe / Renew](#)

FOR CONTRIBUTORS

[Author Guidelines](#)
[For Referees](#)
[OnlineOpen](#)
[Submit an Article](#)

ABOUT THIS JOURNAL

[Contact](#)
[Editorial Board](#)
[Advertise](#)
[Overview](#)

SPECIAL FEATURES

[Cover Gallery](#)
[Read Cover Story](#)

Energy Technology

Generation, Conversion, Storage, Distribution

Energy Technology

© WILEY-VCH Verlag GmbH & Co. KGaA, Weinheim



Impact Factor: 2.824

ISI Journal Citation Reports © Ranking: 2014: 31/89 (Energy & Fuels)

Online ISSN: 2194-4296

Associated Title(s): [Advanced Energy Materials](#), [Chemical Engineering & Technology](#), [Chemie Ingenieur Technik](#), [ChemSusChem](#)

SEARCH


In this journal

[Advanced](#) > [Saved Searches](#) >





SEARCH BY CITATION

Volume: Issue: Page:

Editorial Board

 **Reza S. Abhari**, ETH Zürich **Jim Yang Lee**, National University of Singapore **Fernando Mancilla-David**, University of Colorado, Denver **Götz Vesper**, University of Pittsburgh, PA











Advisory Board

 **Rakesh Agrawal**, Purdue University, West Lafayette, IN **Thomas Aicher**, Fraunhofer-Institut für Solare Energiesysteme, Freiburg **Xinhe Bao**, Dalian Institute of Chemical Physics **János M. Béer**, Massachusetts Institute of Technology, Cambridge **Sally M. Benson**, Stanford University **Gabriele Centi**, Università degli Studi di Messina **James A. Dumesic**, University of Wisconsin, Madison **Vasilis Fthenakis**, Columbia University, New York and Brookhaven National Laboratory, Upton, NY **Muhammad M. Hussain**, King Abdullah University of Science and Technology, Thuwal **George W. Huber**, University of Wisconsin, Madison **Frederik C. Krebs**, Danmarks Tekniske Universitet, Roskilde **Sunggyu Lee**, Ohio University, Athens **Henrik Leion**, Chalmers tekniska högskola, Göteborg **Can Li**, Dalian Institute of Chemical Physics **Ennio Macchi**, Politecnico di Milano **Kazuhiro Mae**, Kyoto University

Chemistry
that
delivers...
Continuous
product
innovation

Create
Innovate
Inspire

WILEY-VCH
WILEY

-  Samuel S. **Mao**, University of California, Berkeley
-  Bernd **Meyer**, TU Bergakademie Freiberg
-  Christoph **Müller**, ETH Zürich
-  Petr **Novák**, Paul-Scherrer-Institut, Villigen
-  Thomas Justus **Schmidt**, Paul-Scherrer-Institut, Villigen
-  Toshimasa **Takanohashi**, Nat'l Inst. of Advanced Industrial Science and Technology, Tsukuba
-  Venkataraman **Thangadurai**, University of Calgary
-  Eric **Wachsman**, University of Maryland, College Park
-  Thomas **Wetzel**, Karlsruher Institut für Technologie
-  Karl-Friedrich **Ziegahn**, Karlsruher Institut für Technologie

Wiley Online Library

Publications

[About Us](#)

Browse by Subject

[Help](#)

[Contact Us](#)

Resources

[Agents](#)

[Advertisers](#)

[Media](#)

[Privacy](#)

[Cookies](#)

[Terms & Conditions](#)

[Site Map](#)






Copyright © 1999-2015 John Wiley & Sons, Inc. All Rights Reserved.

[About Wiley](#) [Wiley.com](#) [Wiley Job Network](#)

WILEY

Your Doorway to
Groundbreaking ResearchAccess research articles for free wileyonlinelibrary.com/journalresourcesWiley
Online
Library[Home](#) > [Chemical Engineering](#) > [General & Introductory Chemical Engineering](#) > [Energy Technology](#) > [Vol 2 Issue 3](#)

JOURNAL TOOLS

-  [Get New Content Alerts](#)
-  [Get RSS feed](#)
-  [Save to My Profile](#)
-  [Get Sample Copy](#)
-  [Recommend to Your Librarian](#)

JOURNAL MENU

[Journal Home](#)

FIND ISSUES

[Current Issue](#)
[All Issues](#)

FIND ARTICLES

[Early View](#)
[Most Accessed](#)
[Most Cited](#)

GET ACCESS

[Subscribe / Renew](#)

FOR CONTRIBUTORS

[Author Guidelines](#)
[For Referees](#)
[OnlineOpen](#)
[Submit an Article](#)

ABOUT THIS JOURNAL

[Contact](#)
[Editorial Board](#)
[Advertise](#)
[Overview](#)

SPECIAL FEATURES

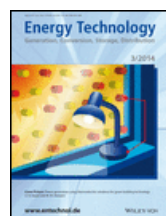
[Cover Gallery](#)
[Read Cover Story](#)

Energy Technology

Generation, Conversion, Storage, Distribution

Energy Technology

© WILEY-VCH Verlag GmbH & Co. KGaA, Weinheim



March 2014

Volume 2, Issue 3
Pages 221–300

[Previous Issue](#) | [Next Issue](#)

Select All

Cover Picture

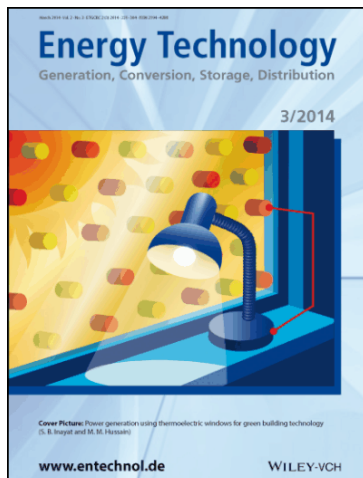
Jump to...

[Top of page](#)
[Cover Picture](#)
[Graphical Abstract](#)
[Review](#)
[Full Papers](#)
[Book Review](#)



Cover Picture: Manufacturing of Thermoelectric Nanomaterials ($\text{Bi}_{0.4}\text{Sb}_{1.6}\text{Te}_3/\text{Bi}_{1.75}\text{Te}_{3.25}$) and Integration into Window Glasses for Thermoelectricity Generation (Energy Technol. 3/2014) (page 221)

Dr. Salman B. Inayat, Kelly R. Rader and Prof. Muhammad M. Hussain
Article first published online: 14 MAR 2014 | DOI: 10.1002/ente.201490004



Thermoelectric windows: A thermoelectric generator is embedded into a window glass that can generate 300 Watts of power at a temperature difference of 20 °C, achieving a new breakthrough in green building technology, as described in the Full Paper by Prof. Muhammad M. Hussain and colleagues at the King Abdullah University of Science and Technology on [page 292](#). Forty percent of global energy consumption is related to room heating and cooling. Therefore, thermoelectric generators integrated into building materials can generate thermoelectricity based upon the temperature difference between the outside temperature and inside building temperature. One major challenge is to have a thermopile that is thick enough (at the least 5 mm in alignment with standard glass thickness). The micrometer-sized thermoelectric powders were therefore ball milled into nanostructured materials and then hot pressed into a mold to form 5 mm thermopiles before inserting into the window glass to make thermoelectric windows.

[Abstract](#) | [Full Article \(HTML\)](#) | [Enhanced Article \(HTML\)](#) | [PDF\(500K\)](#)
[Request Permissions](#)

SEARCH

In this issue

[Advanced](#) > [Saved Searches](#) >

SEARCH BY CITATION

Volume: Issue: Page:

Wiley Journal
Highlights from
2015 Journal
Citation Report

6,500,000+
Journal
articles

1,500+
Journals

240 journals ranked
Top 10 across
JCR categories

1,200 Journals with
JCR Impact Factor

5,786,843
JCR citations to
Wiley journals in 2014

Click to find
out more

Graphical Abstract

[Top of page](#)
[Cover Picture](#)
[Graphical Abstract](#)
[Review](#)
[Full Papers](#)
[Book Review](#)

Graphical Abstract: Energy Technol. 3/2014 (pages 223–226)

Article first published online: 14 MAR 2014 | DOI: 10.1002/ente.201490005

Abstract | **PDF(1031K)** | **Request Permissions**

Review

[Top of page](#)
[Cover Picture](#)
[Graphical Abstract](#)
[Review](#)
[Full Papers](#)
[Book Review](#)

Overview of Design Issues in Product-Integrated Photovoltaics (pages 229–242)

Georgia Apostolou and Prof. Angèle H. M. E. Reinders

Article first published online: 5 MAR 2014 | DOI: 10.1002/ente.201300158



Photovoltaic products: Product-integrated PV (PIPV) is applicable to power ranges from several milliwatts, for PV chargers like the one which is indicated in the figure, up to hundreds of kilowatts for solar vehicles. It is expected that PIPV will be further developed in the forthcoming years and new PV products for both indoor and outdoor use will be released to the market, and here the current status is reviewed.

Abstract | **Full Article (HTML)** | **Enhanced Article (HTML)** | **PDF(1367K)**
References | **Request Permissions**

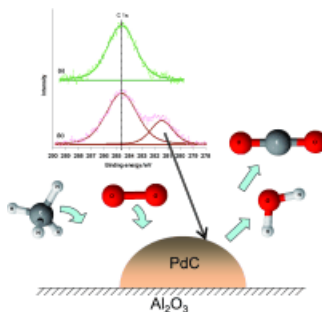
Full Papers

[Top of page](#)
[Cover Picture](#)
[Graphical Abstract](#)
[Review](#)
[Full Papers](#)
[Book Review](#)

Evidence of the Formation of Surface Palladium Carbide during the Catalytic Combustion of Lean Methane/Air Mixtures (pages 243–249)

Adi Setiawan, Prof. Eric M. Kennedy, Prof. Bogdan Z. Dlugogorski, Prof. Adesoji A. Adesina, Olga Tkachenko and Prof. Michael Stockenhuber

Article first published online: 5 MAR 2014 | DOI: 10.1002/ente.201300119



Lean on methane: The catalytic combustion of lean methane/air mixtures over palladium-based catalysts is investigated and the influence of operating parameters and pretreatment conditions on the activity and stability of the catalysts is studied. Significant differences were observed in the light-off temperatures and extent of coke deposition, depending on whether the catalysts were conditioned under oxidizing or reducing conditions.

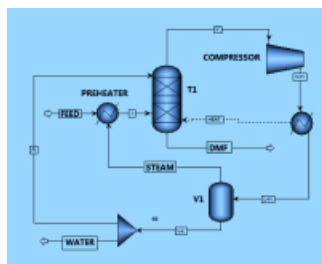
Abstract | **Full Article (HTML)** | **Enhanced Article (HTML)** | **PDF(519K)**
References | **Supporting Information** | **Request Permissions**

Application of Three-Vapor Recompression Heat-Pump Concepts to a Dimethylformamide–Water Distillation Column for Energy Savings (pages 250–256)

Xiaoxin Gao, Prof. Zhengfei Ma, Jiangquan Ma and Limin Yang

Article first published online: 3 MAR 2014 | DOI: 10.1002/ente.201300141

Compressive results: An *N,N*-dimethylformamide (DMF)/water mixture is selected to analyze several distillation-assisted mechanical vapor-recompression (MVR) heat-pump processes compared to conventional

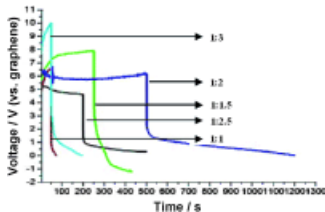


distillation. Four distillation process designs are simulated by using the Aspen software platform to determine the energy savings and best alternative.

[Abstract](#) | [Full Article \(HTML\)](#) | [Enhanced Article \(HTML\)](#) | [PDF\(763K\)](#)
[References](#) | [Request Permissions](#)

Hybrid Composites of LiMn_2O_4 –Graphene as Rechargeable Electrodes in Energy Storage Devices (pages 257–262)

K. V. Sreelakshmi, Soorya Sasi, Dr. A. Balakrishnan, Dr. N. Sivakumar, Dr. A. Sreekrumar Nair, Dr. Shantikumar V. Nair and Dr. K. R. V. Subramanian
 Article first published online: 26 FEB 2014 | DOI: 10.1002/ente.201300120



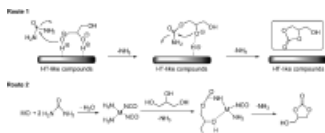
Composite results: This paper details the synthesis of spinel-lithium manganese oxide (LiMn_2O_4) powders by using a simple sol–gel method with polyvinyl alcohol (PVA), and further combination with a conductive additive, graphene, to produce a composite electrode material for simultaneously improving power density (current Li-ion batteries have low power density as a disadvantage) along with

energy density.

[Abstract](#) | [Full Article \(HTML\)](#) | [Enhanced Article \(HTML\)](#) | [PDF\(845K\)](#)
[References](#) | [Supporting Information](#) | [Request Permissions](#)

A Sustainable Preparation of Glycerol Carbonate from Glycerol and Urea Catalyzed by Hydrotalcite-Like Solid Catalysts (pages 263–268)

Yongfa Sun, Dr. Xinli Tong, Zhidong Wu, Jinbiao Liu, Yongtao Yan and Song Xue
 Article first published online: 26 FEB 2014 | DOI: 10.1002/ente.201300135



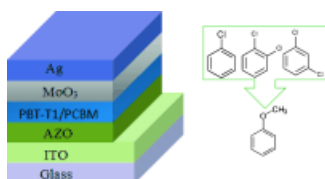
Selective synthesis: The selective synthesis of glycerol carbonate from glycerol and urea catalyzed by hydrotalcite-like compounds is performed under solvent-free conditions, and that such compounds including Mg, Zn, and Al elements have very high catalytic activity. As a

result, high conversion and selectivity for glycerol carbonate are obtained under suitable conditions.

[Abstract](#) | [Full Article \(HTML\)](#) | [Enhanced Article \(HTML\)](#) | [PDF\(411K\)](#)
[References](#) | [Request Permissions](#)

Polymer Solar Cells Processed Using Anisole as a Relatively Nontoxic Solvent (pages 269–274)

Swaminathan Venkatesan, Dr. Qiliang Chen, Evan C. Ngo, Nirmal Adhikari, Kelly Nelson, Ashish Dubey, Jianyuan Sun, Prof. Venkateswara Bommesetty, Prof. Cheng Zhang, Prof. David Galipeau and Prof. Qiquan Qiao
 Article first published online: 26 FEB 2014 | DOI: 10.1002/ente.201300174



Detoxifying photovoltaics: A relatively nontoxic single solvent, anisole, was successfully demonstrated to process organic photovoltaics, thereby decreasing the risk to human health for large-scale production. The photo-charge extraction by linearly increasing voltage (photo-CELIV) and transient photocurrent/photovoltage measurements

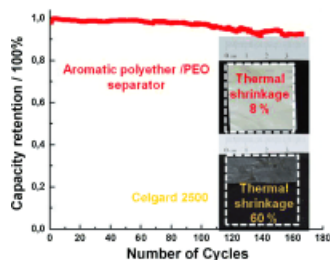
were used to characterize the devices.

[Abstract](#) | [Full Article \(HTML\)](#) | [Enhanced Article \(HTML\)](#) | [PDF\(581K\)](#)
[References](#) | [Request Permissions](#)

Large-Scale Separators Based on Blends of Aromatic Polyethers with PEO for Li-Ion Batteries: Improving Thermal Shrinkage and Wettability Behavior (pages 275–283)

Dr. Valadoula Deimede, Dr. Andrea Voegelé, Dr. Georgia Lainioti, Dr. Costas Elmasides and Prof. Joannis K. Kallitsis
 Article first published online: 3 MAR 2014 | DOI: 10.1002/ente.201300153

Large-scale separators: The development of large-scale separators with tuned microstructures is presented for application to



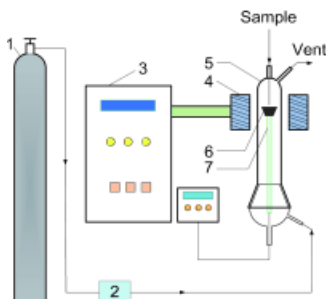
Li-ion batteries. Porous separators based on blends of aromatic polyethers and polyethylene oxide (PEO) are obtained, showing much improved thermal shrinkage and wettability behavior compared to the commercial separator.

[Abstract](#) | [Full Article \(HTML\)](#) | [Enhanced Article \(HTML\)](#) | [PDF\(1463K\)](#)
[References](#) | [Supporting Information](#) | [Request Permissions](#)

Comparison of Structure and Gasification Reactivity of Rapid Pyrolysis Chars of Coal Water Slurries and Parent Coals (pages 284–291)

Zhijie Zhou, Lu Ding, Lei Wu, Shanjun Lin, Tongmin Cui, Prof. Guangsuo Yu and Prof. Fuchen Wang

Article first published online: 3 MAR 2014 | DOI: 10.1002/ente.201300172



Coal hard results: Rapid pyrolysis of coal-water slurries (CWS) and parent coals are performed in a drop-style high-frequency furnace. The results show that, as the pyrolysis temperature increases, the char pyrolysis yields differ between CWS and parent coals, in which there is a competition between steam reaction with coal/char and water evaporation in the process.

[Abstract](#) | [Full Article \(HTML\)](#) | [Enhanced Article \(HTML\)](#) | [PDF\(712K\)](#)
[References](#) | [Request Permissions](#)

Manufacturing of Thermoelectric Nanomaterials ($\text{Bi}_{0.4}\text{Sb}_{1.6}\text{Te}_3/\text{Bi}_{1.75}\text{Te}_{3.25}$) and Integration into Window Glasses for Thermoelectricity Generation (pages 292–299)

Dr. Salman B. Inayat, Kelly R. Rader and Prof. Muhammad M. Hussain

Article first published online: 26 FEB 2014 | DOI: 10.1002/ente.201300166



More than a window: Until now thermoelectric generators have been built on a single side of a substrate, therefore requiring the two temperature environments to exist on the same side of the substrate. Here, thermoelectric nanomaterials are embedded into window glass to generate thermoelectricity from the temperature gradient between the solar-heated outdoors and the relatively cold

indoor temperature.

[Abstract](#) | [Full Article \(HTML\)](#) | [Enhanced Article \(HTML\)](#) | [PDF\(1718K\)](#)
[References](#) | [Supporting Information](#) | [Request Permissions](#)

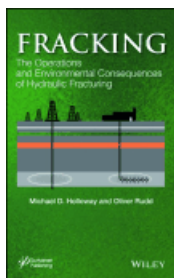
Book Review

[Top of page](#)
[Cover Picture](#)
[Graphical Abstract](#)
[Review](#)
[Full Papers](#)
[Book Review](#)

Fracking: The Operations and Environmental Consequences of Hydraulic Fracturing. By Michael D. Holloway and Oliver Rudd (page 300)

Prof. Roger E. Kasperson

Article first published online: 26 FEB 2014 | DOI: 10.1002/ente.201405001



Scrivener Publishing, Beverly, MA, 2013; 366 pp., hardcover, €169.00—ISBN 978-1-118-49632-9

[Abstract](#) | [Full Article \(HTML\)](#) | [Enhanced Article \(HTML\)](#) | [PDF\(192K\)](#)
[Request Permissions](#)

Select All

Wiley Online Library

Publications

[About Us](#)

Browse by Subject

[Help](#)

[Contact Us](#)

Resources

[Agents](#)

[Advertisers](#)

[Media](#)

[Privacy](#)

[Cookies](#)

[Terms & Conditions](#)

[Site Map](#)

Copyright © 1999-2015 John Wiley & Sons, Inc. All Rights Reserved.

[About Wiley](#)

[Wiley.com](#)

[Wiley Job Network](#)

WILEY

Evidence of the Formation of Surface Palladium Carbide during the Catalytic Combustion of Lean Methane/Air Mixtures

Adi Setiawan,^[a] Eric M. Kennedy,^[a] Bogdan Z. Dlugogorski,^[a] Adesoji A. Adesina,^[b] Olga Tkachenko,^[c] and Michael Stockenhuber*^[a]

The catalytic combustion of < 1 % methane in air over palladium-based catalysts is investigated. The influence of operating parameters and pretreatment conditions on the activity and stability of the catalysts is studied. X-ray photoelectron spectroscopy analysis of Pd/Al₂O₃ indicates the emergence of Pd carbide, even under lean conditions (0.6 % methane) and at temperatures as low as 180 °C. Significant differences were observed in the light-off temperatures and extent of coke

deposition, depending on whether the catalysts were conditioned under oxidizing or reducing conditions. The oxidized palladium catalysts were reduced by methane under reaction conditions and exhibited similar activity compared to catalysts which were activated under hydrogen. Time-on-stream experiments reveal that the stability of the Pd/Al₂O₃ catalyst reduced in hydrogen was only marginally improved compared to catalysts calcined in air.

Introduction

Methane is a gas with a GHG potential which is 23 times greater than that of CO₂^[1] and under certain circumstances the oxidation of methane to CO₂ is considered a viable option to reduce net greenhouse gas emissions, especially when the concentration of methane is well below its lower explosion limit of 5%. Catalytic oxidation of methane is one of the most promising technologies to mitigate methane emissions as it can operate under a wide range of methane concentrations and at low reaction temperatures. The relatively low temperature of catalytic combustion for lean methane streams is an important advantage over other combustion technologies because of its potential to achieve a significant reduction in energy usage due to minimal heat losses from the process, significantly reduced requirements for the addition of fuel to the process as well as limited reaction of most contaminants with the solid catalyst. High conversion at high space velocities can be achieved, which, in turn, reduces the reactor size compared to high temperature combustion technology.

Palladium catalysts are well known to be highly active catalytic materials for the total combustion of methane. These catalysts exhibit high activity for oxidation of alkanes at low temperatures, especially when supported on high surface area oxides such as γ -alumina. The high specific surface area of the support enables high metal dispersion which, in turn, results in high catalytic activity.^[2] A wide range of research has been performed in recent years to investigate the oxidation behaviour and catalytic properties of metal oxides^[3] and noble-metal-based catalysts, with a number of comprehensive reviews published in this area.^[2,4] Recently, supported palladium catalysts were investigated experimentally in a laboratory-scale monolithic reactor study and also by simulation,^[5,6]

with the aim of developing more cost effective and efficient catalytic combustion technologies.^[6]

It is generally agreed that catalyst pretreatment plays an important role in controlling the activity and durability of catalysts. Under oxygen-rich conditions, for palladium catalysts, it is suggested that PdO is formed and this phase represents the active phase for methane oxidation.^[2] Other investigators claim that reduced Pd was an important active site for the catalytic combustion reaction,^[7–9] whereas others have suggested that the surface structure of the Pd-based catalysts changes with time-on-stream under fuel-rich conditions.^[10]

Although the coking of transition-metal catalysts was reported during the combustion of methane at higher concentrations^[11,12] and reaction temperatures,^[12] we have observed the formation of significant quantities of carbonaceous material under highly oxygen-rich conditions which, to our knowledge, has not been previously reported. Furthermore, we

[a] A. Setiawan, Prof. E. M. Kennedy, Prof. B. Z. Dlugogorski, Prof. M. Stockenhuber
Priority Research Centre for Energy (PRCfE)
School of Engineering
University of Newcastle
Callaghan, NSW, 2308 (Australia)
E-mail: Michael.Stockenhuber@newcastle.edu.au

[b] Prof. A. A. Adesina
Reaction Engineering and Technology Group
School of Chemical Engineering
University of New South Wales
Kensington, Sydney, NSW, 2052 (Australia)

[c] O. Tkachenko
Russian Academy of Sciences
N.D. Zelinsky Institute of Organic Chemistry
Moscow (Russian Federation)

Supporting information for this article is available on the WWW under <http://dx.doi.org/10.1002/ente.201300119>.

have observed that methane can be activated at temperatures as low as 180 °C, which could have important consequences for the development of technologies for the low temperature catalytic combustion of methane.

The dependency of light-off curves and overall catalytic activity depends on the pretreatment history of catalysts and the deactivation behaviour needs further investigation in order to improve the performance of the catalytic system. Moreover, the chemical nature of carbon deposits, identified as Pd carbide^[13] formed under reaction conditions is under debate.^[14]

In this study, we examined the effect of pretreatment conditions on the activity of a catalyst based on palladium supported on aluminium for combustion of air mixtures containing low concentrations of methane (0.2–0.8%). We observed the formation of carbonaceous deposits and were able to correlate coke deposition with catalyst activation procedures. We also examined catalyst deactivation during time-on-stream methane combustion experiments undertaken in conditions where the level of methane conversion was over 90%.

Results and Discussion

Catalytic activity

Pretreatment procedures were varied for the 1.2 wt% Pd/Al₂O₃ catalysts in order to examine the effect of oxygen and hydrogen pretreatment on the catalytic activity. The methane conversion curves obtained from these samples are plotted in Figure 1. At lower temperatures (below 280 °C), the catalyst activated in air shows a higher conversion level compared to the sample reduced in hydrogen. At temperatures higher than T_{50} (temperature at 50% conversion), the activity of both samples was essentially the same. In addition, the calcined–reduced sample demonstrates the same activity during

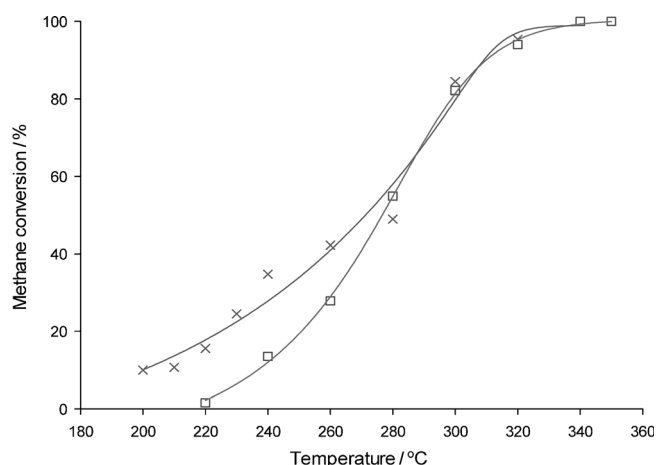


Figure 1. Methane conversion over 1.2 wt% Pd/Al₂O₃ catalysts activated in air–He–H₂ (calcined–reduced) and activated in air (calcined). Inlet mixture: 6000 ppm CH₄ in air, 250 mg catalyst, GHSV = 33 000 h⁻¹. x = calcined sample, □ = calcined–reduced sample.

heating and cooling cycles, that is, showing no hysteresis (see Figure A.2 of the Supporting Information).

The surface area of a 1.2 wt% Pd/Al₂O₃ catalyst decreased after reaction, suggesting pore-blocking of the support (see Table 1). Consistent with our carbon balance analysis, we

Table 1. BET Surface area.

Sample	Surface area [m ² g ⁻¹]
alumina, 99%	63.7
0.1 wt.% Pd/Al ₂ O ₃ , fresh	61.1
1.2 wt.% Pd/Al ₂ O ₃ , fresh	58.6
1.2 wt.% Pd/Al ₂ O ₃ , used	47.5

suggest that methane is reducing the Pd species under our reaction conditions and forming carbonaceous deposits. The existence of these deposits has been substantiated using X-ray photoelectron spectroscopy (XPS) analysis (see below). At higher temperatures (once the Pd is reduced), these deposits are removed as indicated by the observation of a carbon balance in excess of 100% at elevated temperatures.

It is suggested that a low-oxidation-state palladium species is formed at higher temperatures, which is the active phase for complete oxidation. The oxidized Pd can activate methane as indicated by the high conversion at temperatures below 350 °C. The presence of PdO at lower temperatures has been reported in the published literature where it was suggested that the oxidized PdO phase is more active compared to its reduced form.^[10] Without a separate reduction step, PdO starts reacting with methane at T_{10} = 180 °C whereas, over a hydrogen-reduced Pd/Al₂O₃ catalyst, a similar conversion is achievable only at temperatures ≥ 220 °C.^[10]

Figure 2 shows the methane conversion and carbon-balance changes of methane-oxidation experiments over Pd/

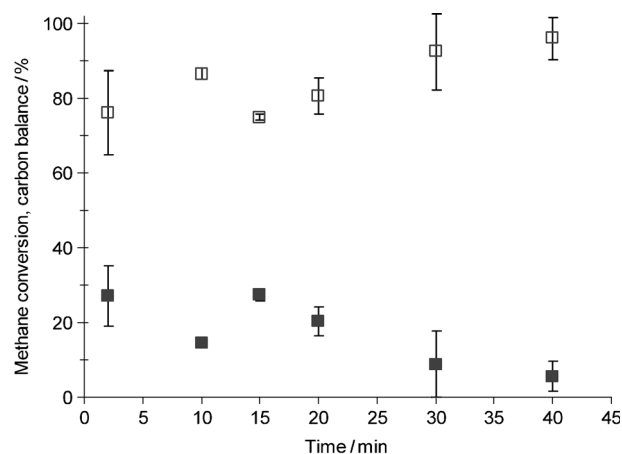


Figure 2. Carbon balance and methane conversion as a function of time during methane oxidation over 1.2 wt% Pd/Al₂O₃ catalysts at 180 °C. The sample was pretreated in air at 500 °C for 1 h. Inlet mixture: 5000 ppm CH₄ in air, 250 mg catalyst, GHSV = 33 000 h⁻¹. ■ = methane conversion; □ = carbon balance.

Al₂O₃ catalyst at a reaction temperature of 180 °C in which the feed is 5000 ppm CH₄ in air. To illustrate the differences in carbon balance at low and high temperatures the analyzed concentrations are compared in Figure A3 of the supplementary section. These data support the argument that CH₄ is adsorbed and reacts on the catalyst to form carbonaceous species at lower temperatures consistent with the observed deficit in the mass balance. Along with a decrease in methane conversion, the carbon balance increases with time on stream, and approaches 100% at 180 °C. This indicates that, after 40 min on stream, maximum coverage with coke is observed. The formation of coke is quite surprising, because only 0.5% methane was present in the air and it is evident that methane is being activated at a very low temperature. The amount of coke deposited at 180 °C corresponds to approximately $1 \times 10^{-5} \text{ mol}_C \text{ g}^{-1}$ of catalyst, compared with a loading of surface Pd species (based on Pd3d_{5/2} photoelectrons) of $4 \times 10^{-5} \text{ mol}_{Pd} \text{ g}^{-1}$ of catalyst. Thus, only a fraction of accessible Pd is covered by coke and, consequently, only a fraction was involved in methane activation at low temperatures. To determine the fate of the carbon species deposited, spent catalyst was heated in zero-air from 400 °C to 800 °C; CO₂ was detected in the outlet of the reactor, suggesting the existence of coke on the catalyst. The CO₂ was quantified and the balance with the deposited carbon was approximately 96% (relative), suggesting that all the carbon could be removed by heating in air at 400 °C. The existence of carbon deposits was further substantiated by thermal gravimetric analysis (TGA) and total organic carbon analysis (TOC). Carbon deposition on Pd catalysts with methane has been reported before at low temperatures by Dropsch and Baerns, but only under higher methane concentrations (20% CH₄ balanced He).^[15]

It is interesting to note that, at higher temperatures (350 °C), we observed only minor catalyst deactivation of palladium supported on alumina catalyst in the time on stream experiment. There was only a 5% drop in methane conversion from 100% conversion observed over a period of 35 h for the catalyst calcined in air (Figure 3, inlet methane = 6000 ppm). It should be noted that the catalyst was operating at close to 100% conversion. However, a significant level of deactivation was observed at lower space velocities and temperatures during time-on-stream experiments using the Pd catalyst (see Figure A.4 in the Supporting Information). It was explained that the deactivation with time on stream is due to transformation of active sites (PdO) into less active sites, Pd(OH)₂,^[16,17] which can be a result of poisoning of the active sites by H₂O produced by the reaction. By purging the deactivated catalyst in a dry carrier gas stream above 500 °C, the initial catalytic activity was at least partially restored.

We also observed hydrogen in the product stream of this reactivation process, confirming the reverse decomposition of Pd(OH)₂ into a PdO phase. This is in agreement with what has been reported by Roth et al. and Castellazzi et al.^[18,19]

Methane conversion as a function of reaction temperature at different values of gas hourly space velocity (GHSV) as

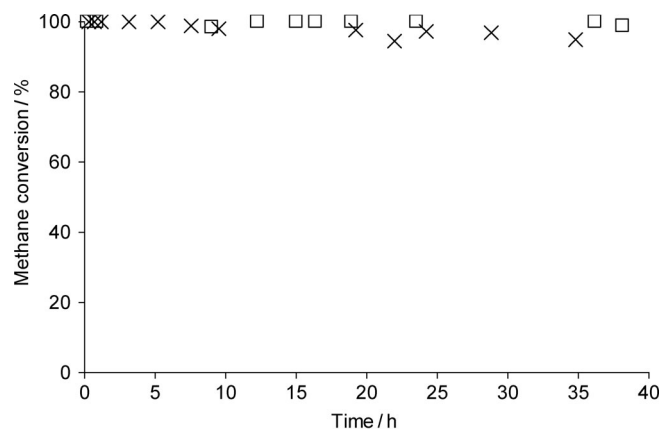


Figure 3. Evaluation of time-on-stream behavior at 350 °C over 1.2 wt.% Pd/Al₂O₃ catalysts, feed = 6000 ppm CH₄ in air with a space velocity of 33 000 h⁻¹. □ = catalyst was activated in air and subsequently reduced in hydrogen (300 °C); × = calcined in air (500 °C).

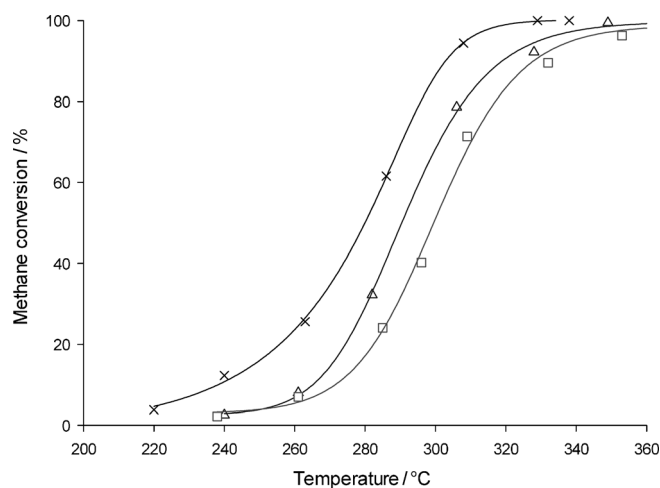


Figure 4. Methane conversion over Pd/Al₂O₃ catalysts as a function of temperature at various space velocities. Feed: 8000 ppm CH₄ in air. Activated in air at 500 °C for 1 h, purged with He for 30 min at 300 °C and reduced in H₂ at 300 °C for 2 h. × = 50 000 h⁻¹; Δ = 80 000 h⁻¹; □ = 200 000 h⁻¹.

shown in Figure 4 indicates that the Pd-based catalysts remain active, even at very high space velocities. The light-off temperature (T_{10} , the temperature in which noticeable oxidation occurs) at a gas velocity of 50 000 h⁻¹ was 240 °C, whereas, at higher space velocities and at the same temperature, there is no significant methane conversion. At 50 000 h⁻¹, maximum conversion was achieved at the reaction temperature of 330 °C, whereas the air-methane mixture at a GHSV of 80 000 h⁻¹ requires temperatures of up to 350 °C for complete combustion. In addition, when the space velocity was increased up to 200 000 h⁻¹, the level of highest conversion of methane was achieved at 370 °C. In the temperature range between 280 °C and 320 °C, an almost linear dependency of the conversion with space velocity was observed, similar to what others have reported in methane oxidation over magnesium- and manganese-supported catalysts in plug flow reactors.^[20,21] The methane combustion outside

this temperature range is likely to become mass or heat transfer controlled.^[4]

The effect of palladium loading on the catalytic combustion was investigated using 0.1 wt % and 1.2 wt % Pd supported on gamma alumina catalysts (see the Supporting Information, Figure A.5). In this experiment, the inlet methane concentration was set at 6000 ppm and the flow rate and GHSV were maintained at 33000 h⁻¹. It was found by Cullis and Willatt that the loading of precious metal on the support contributes significantly to catalyst activity at much higher CH₄ concentration.^[22] The light-off temperature of a feedstock containing 0.6% methane in air is much lower over 1.2 wt % Pd compared to the 0.1 wt % Pd/Al₂O₃ catalyst (see the Supporting Information). Low conversion of methane over 0.1% loading was observed at 300 °C; however, on using 1.2 wt % Pd/Al₂O₃ catalyst at this temperature, 80% methane was converted to CO₂. Estimation of the turnover number suggested a significant difference in activity between the catalysts, 4 × 10⁻² s⁻¹ at 250 °C for 1.2% Pd (GHSV = 200000 h⁻¹) and 9.5 × 10⁻³ s⁻¹ for 0.1% Pd (GHSV = 10000 h⁻¹). Conversion over both catalysts was below 5%. This difference in activity is consistent with previous studies^[19,23] and suggests a variation of the chemical properties of the active sites which is influenced by the loading and particle size. Even at the low methane concentrations used in this study, a clear trend of increased activity with catalyst loading is observed. Interestingly, the sample with lower palladium loading also shows rapid deactivation at temperatures higher than 450 °C. Over this catalyst, 100% oxidation could not be achieved at temperatures as high as 650 °C.

The nature of the sites active in methane combustion

In general, the specific surface areas of all samples were in the range of 50–60 m² g⁻¹ as listed in Table 1. An increase in the palladium loading decreased the surface area of the catalyst slightly. The used 1.2 wt % Pd/Al₂O₃ catalyst has a Brunauer–Emmett–Teller (BET) surface area of 47.5 m² g⁻¹ whereas the fresh sample exhibits a surface area of 58.6 m² g⁻¹, disclosing a 19% loss of surface area of the Pd/Al₂O₃ catalyst during methane oxidation.

XRD patterns of palladium-based catalysts, in comparison with γ - δ alumina, reveal minute Pd or PdO reflections (identified by slightly increased intensities and widths of reflections from the support) consistent with the low metal-loading and the highly dispersed nature of the palladium particles on the support. H₂-chemisorption analysis suggested a dispersion level of 68% for the palladium calcined in air (see Supporting Information). Based on this measurement, it is estimated that the average size of active palladium particles is 1.6 nm.

This is consistent with the XRD result. For Pd/Al₂O₃ reduced in H₂, the dispersion decreases to 9% and the average particle diameter to 12.2 nm. This lower dispersion level is likely due to sintering of Pd in the hydrogen atmosphere, which is substantiated by TEM measurements as reported in the Supporting Information. The images of the palladium samples suggest that the palladium particle size of the reduced sample is larger than the calcined Pd/Al₂O₃ (see Figure A.6, A.7 of Supporting Information).

Figure 5a displays Pd3d spectra of Pd/Al₂O₃ catalyst calcined in air and subsequently reduced in hydrogen. Based on the peak shape of the Pd3d peak, the presence of two Pd

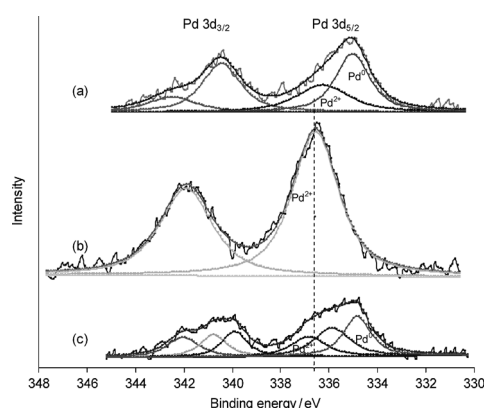


Figure 5. XPS spectra of Pd3d core level region of Pd/Al₂O₃ catalysts, (a) calcined–reduced sample, (b) calcined sample, (c) coked sample.

species in the reduced (H₂-treated) catalyst can be suggested. Fitting the Pd3d_{5/2} peak to a Gaussian Lorentzian curve results in two different photoelectron binding energies (BE) of 335.0 eV (Pd3d_{5/2} core level) and 336.3 eV (Pd3d_{5/2} core level). In Table 2, the species, atom percentage, and Pd/Al ratio are summarized. The chemical species exhibiting the peak at 336.3 eV is identified as Pd²⁺.^[24] The BE peak position at 335.0 eV of the second peak of the reduced sample suggests formation of Pd⁰ (metallic palladium clusters), similar to the XPS results reported by Tompos and co-workers.^[25] As illustrated in Figure 5b, for calcined Pd/Al₂O₃, the peaks are more intense and slightly broader (Pd3d_{5/2}) and fitting an

Table 2. XPS peak position and surface composition of Pd/Al₂O₃ catalysts.

Sample	Peak position Pd 3d _{5/2} [eV]	Species and atom percentage	Atomic surface ratio Pd/Al
calcined–reduced Pd/Al ₂ O ₃	335.0	(Pd ⁰) 59%	0.0046
	336.3	(Pd ²⁺) 41%	
calcined Pd/Al ₂ O ₃	336.6	(Pd ²⁺) 100%	0.0055
coked Pd/Al ₂ O ₃	334.9	(Pd ⁰) 40%	0.0047
	335.9	(Pd ²⁺) 36%	
	336.9	(Pd ²⁺) 24%	

additional peak did not result in significant decrease of χ^2 of the overall fit. Thus, only a single peak was fitted for Pd3d_{5/2} and Pd3d_{3/2}, at BEs of 341.9 eV and 336.6 eV, respectively. It is inferred that, after activation in air, only one Pd species exists on the surface.

In Figure 5c, the X-ray photoelectron spectrum of a coked sample reveals three different species at 334.9 eV, 335.9 eV, and 336.9 eV (Pd3d_{5/2} core level), suggesting reaction of Pd²⁺ upon low-temperature treatment of the oxidized Pd sample with methane and resulting in the formation of an additional Pd²⁺ species and a Pd⁰ species. This coked sample was activated in air only.

It may be noted that the binding energy of the Pd3d_{5/2} peak identified as Pd²⁺ changed from 336.6 eV to 336.9 eV compared to the precursor sample, that is, the sample calcined in air. This BE change can be related to the formation of carbonaceous compound in the vicinity of the Pd²⁺ species or changes in the particle size. The Pd3d_{5/2} peak at 335.9 eV can be attributed to PdC_x, which has been reported previously.^[26] The values of BE in the present study are observed to be at a slightly higher energies than corresponding literature values. BE changes in small noble metal particles are not only a result of the oxidation state but also the surrounding atoms (due to changes in the Madelung potential and relaxation).^[27,28] Meanwhile, the peak at BE of 334.9 eV is consistent with Pd⁰ peak position reported in the literature.^[25,26] This is a very low temperature for reduction of Pd²⁺ to Pd⁰ with methane.^[29,30] We suggest the discrepancy with the literature may be a result of the decomposition of highly active carbide species that have formed at low temperatures (180 °C).

The particle diameter of 1.2 nm and 1.8 nm that were determined in the present study are within the range of significant differences of nanoparticles compared to bulk species.^[31] The difference in BE of the carbide peak compared to the literature^[26] is more likely the result of the smaller particle size or the stoichiometry of PdC_x formed on nanoparticles compared to the single crystal studies. The stoichiometry of the carbide species is also expected to have an influence on the photoelectron lines, which might explain the small differences between the present findings and the literature. Evidence of a carbide species was also found in the C1s spectra (see Figure 6).

The spectra of the C1s core level region of used Pd/Al₂O₃ catalysts are shown in Figure 6. The peak shape and width of the C1s peak suggests that carbon is present in the form of multiple species (coked sample). For clean samples (without coking), a single peak at 284.6 eV can be observed, which is identified as adventitious carbon. For the coked sample, significant peak broadening and a shoulder peak at 281.5 eV was observed. Thus, two peaks were fitted using the same peak shape as above (30:70 Gaussian–Lorentzian) one peak corresponding to adventitious carbon at a BE of 284.6 eV and a peak at BE = 281.5 eV.^[24,32] The peak at 281.5 eV most likely originates from the formation of carbide-like species. We cannot exclude the possibility of aluminium carbide formation, but suggest aluminium carbide formation to be un-

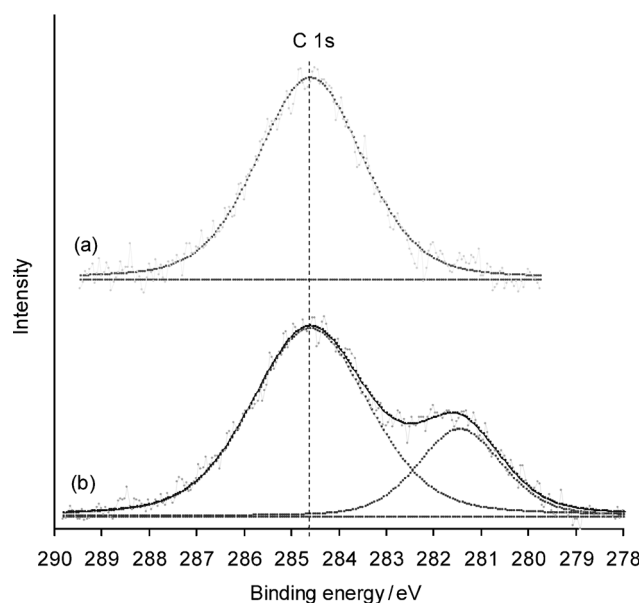


Figure 6. XPS spectra of C1s core level region of used Pd/Al₂O₃ catalysts; (a) without coking, (b) coked sample.

likely, due to a constant FWHM of the Al2p line for the coked and uncoked sample which suggests absence of any aluminium phases other than oxide. In contrast, a Pd3d_{5/2} peak at 335.9 eV was observed in the coked samples, providing further evidence for the formation of a PdC_x phases (see above). The peak position at 281.5 eV is, however, found at slightly lower binding energies than Pd carbide and Al carbides.^[33] The C1s peak formed from CF₂Cl₂ on Pd catalysts was reported^[34] (suggested to be carbide) to be at 282.9 eV, whereas carbon monoxide decomposition over Pd/alumina led to a carbide C1s peak at 282 eV.^[35] This illustrates that significant changes in the BE of carbide species have been reported in the literature and may reflect changes in particle size and also stoichiometry of the carbide phase when compared to data reported in the literature. Pd carbide formation from methane was also inferred from XRD measurements of Pd/Al₂O₃ catalysts,^[36] supporting our assertion of the formation of a carbide species in the present study. Furthermore, we observed an additional peak with a shift of approximate −1.0 eV of the Pd3d_{5/2} BE (Pd²⁺), which is consistent with an increase of the electron density surrounding Pd²⁺ resulting from the formation of carbide. The C1s peak at 281.5 eV could also originate from graphitic species on alumina but the Pd3d_{5/2} peak at 335.9 eV is evidence for the formation of an additional species formed on the surface. The low binding energy of the C1s species suggests that the carbon is negatively charged or bound to an electropositive species such as Pd. More importantly, the presence of an additional C1s peak strongly supports the findings from the reactor studies in which carbon deposition was inferred as the carbon balance and the conversion data presented in Figure 1 and Figure 2. Note that increasing the temperature of the coked sample to 320 °C results in a decrease of the intensity of the C1s peak at 281.7 eV (not shown), suggesting decomposition

of the carbide species which is consistent with the formation of CO₂ upon heating to 400 °C.

Conclusions

Catalysts based on palladium supported on alumina were prepared and activated under controlled conditions. Pd/Al₂O₃ catalysts calcined in air and then reduced in hydrogen exhibit a lower catalytic activity at low temperatures compared to those activated in air only. Interestingly, even under very lean conditions, methane is converted at 180 °C and carbon is formed on palladium catalysts. Upon increasing the reaction temperature, the catalysts are reduced by methane and exhibit similar activity to catalysts reduced with hydrogen. Based on XPS analysis, it is concluded that the carbon formed at 180 °C is most likely present in the form of a Pd-carbide species. Heating the coked sample to 320 °C in air converts the carbide species to CO₂.

Experimental Section

Catalyst Preparation: Catalysts containing 0.1–1.2 wt % Pd were prepared by wet impregnation of an alumina (gamma and delta Al₂O₃, Chem-Supply) support with a Pd(NO₃)₂ solution (10 wt % in 10 wt % nitric acid, Sigma–Aldrich). The dried catalyst (110 °C) was ground, pressed and sieved to 250–400 μm. The solid was then calcined in air at 500 °C (40 mL min⁻¹) for 1 h in a tubular fixed-bed reactor and purged with helium (40 mL min⁻¹) for 30 min. The sample was then reduced in 99.99% H₂ at 300 °C (20 mL min⁻¹) for approximately 2 h and the activation was completed by purging with helium while bringing the temperature to the desired reaction value (calcined–reduced sample). Some Pd/Al₂O₃ catalyst samples were activated at 500 °C for 1 h in air in order to investigate the effect of pretreatment conditions on the catalyst activity (calcined sample).

Catalytic activity measurements: The catalytic measurements were performed using a tubular stainless steel micro reactor. The composition of the reaction mixtures was varied in the range of 0.2–0.8% of CH₄, balanced with air at various flow rates. The inlet and outlet mixture compositions were analyzed using a gas chromatograph equipped with a thermal conductivity detector (TCD) and concentric packed column (Alltech CTR-1). Methane (99.95%) and compressed air flows were adjusted by means of mass flow controllers. Reactor feed and effluent streams were injected on the GC column through a Valco 6-port injection valve. In all experiments, helium was used as a GC carrier gas. Injections were repeated three times and the standard deviation of the conversion was ±3%. No methane conversion was detected when the feed was heated up to 650 °C in the absence of catalyst. Details of the experimental setup are shown in Supporting Information (SI) Figure A.1.

Characterization of catalysts: The surface area of fresh and used catalysts were determined by nitrogen adsorption at 77 K using a Gemini 11 2370 surface area analyser using the BET method. Powder X-Ray diffraction patterns of fresh and used catalysts were examined using CuK_α radiation with a Philips X'Pert diffractometer. Diffractograms were collected in the 2θ angle range from 2° to 90° with 0.008° 2θ step resolution. For surface analysis, ex situ XPS was carried out using AlK_α radiation. The emitted photoelectrons were analyzed using a PHOIBOS 100 hemispherical analyser manufactured by SPECS GmbH. Used

samples were collected immediately after terminating the reaction by cooling in helium and the catalyst was then stored in a sealed container. The sample was mounted on an XPS sample holder using indium tape. The exposure time of samples in air was minimized in order to reduce the likelihood of water adsorption or oxidation of the carbon deposited on the catalyst. The energy scale was shifted relative to the adventitious carbon peak at 284.6 eV. The shift was cross-checked with the position of O 1s from Al₂O₃, which is found at 531 eV. For measuring the metal dispersion of the catalysts, pulse chemisorption experiments utilizing a mixture of 10% H₂ in N₂ were performed at 109.1 °C using Micromeritics 2910 AutoChem (Micromeritics Instruments Corp., USA). TEM images of the sample were taken with a JEOL 2100 TEM.

The elemental composition of the catalyst was determined by inductively coupled plasma optical emission spectrometry (ICP-OES) using a Varian 715 ES spectrometer. Prior to analysis, the sample was dissolved in a solution of 4.5 mL HNO₃ (65%); 4.5 mL HCl (37%); 3 mL HBF₄ (50%) and 600 μL Tm internal standard (1000 ppmv) as added as an internal standard. All samples were then digested using a Milestone Start D Microwave Unit for a minimum time of 2 h. No sample contamination of nitrate was observed (detection limit of 30 ppm, based on the solid).

Acknowledgements

Financial support from ACARP is duly acknowledged. A.S. was sponsored by the Aceh Province Government, Indonesia. We thank Jane Hamson for assistance with ICP analysis and TGA-MS. Thanks are also due to Matthew Drewery and Viswanathan Arcotumapathy for their help with catalyst synthesis and chemisorption analysis, respectively. We are grateful to University of Wollongong (XPS analysis), UN (XRD and TEM analyses at EM/X-ray unit), and the Australian Synchrotron for the use of their facilities.

Keywords: catalysis • combustion • methane conversion • palladium • palladium carbide

- [1] *Climate Change 2007: The Physical Science Basis* (Eds.: S. Solomon, D. Qin, M. Manning, Z. Chen, M. Marquis, K. B. Averyt, M. Tignor, H. L. Miller), Cambridge University Press, Cambridge, **2007**.
- [2] P. Gélin, M. Primet, *Appl. Catal. B* **2002**, *39*, 1–37.
- [3] J. Li, H. Fu, L. Fu, J. Hao, *Environ. Sci. Technol.* **2006**, *40*, 6455–6459.
- [4] J. H. Lee, D. L. Trimm, *Fuel Process. Technol.* **1995**, *42*, 339–359.
- [5] K. Gosiewski, Y. S. Matros, K. Warmuzinski, M. Jaschik, *Chem. Eng. Sci.* **2008**, *63*, 5010–5019.
- [6] S. Su, J. Agnew, *Fuel* **2006**, *85*, 1201–1210.
- [7] S. H. Oh, P. J. Mitchell, R. M. Siewert, *J. Catal.* **1991**, *132*, 287–301.
- [8] R. F. Hicks, H. Qi, M. L. Young, R. G. Lee, *J. Catal.* **1990**, *122*, 280–294.
- [9] M. Lyubovskiy, L. Pfefferle, *Catal. Today* **1999**, *47*, 29–44.
- [10] T. V. Choudhary, S. Banerjee, V. R. Choudhary, *Catal. Commun.* **2005**, *6*, 97–100.
- [11] P. Euzen, J. H. Le Gal, B. Rebours, G. Martin, *Catal. Today* **1999**, *47*, 19–27.
- [12] V. A. de la Peña O'Shea, M. C. Alvarez-Galvan, J. Requies, V. L. Barrio, P. L. Arias, J. F. Cambra, M. B. Güemez, J. L. G. Fierro, *Catal. Commun.* **2007**, *8*, 1287–1292.

- [13] N. Seriani, F. Mittendorfer, G. Kresse, *J. Chem. Phys.* **2010**, *132*, 024711–024718.
- [14] M. W. Tew, M. Nachtegaal, M. Janousch, T. Huthwelker, J. A. van Bokhoven, *Phys. Chem. Chem. Phys.* **2012**, *14*, 5761–5768.
- [15] H. Dropsch, M. Baerns, *Appl. Catal. A* **1997**, *165*, 159–169.
- [16] C. F. Cullis, T. G. Nevell, D. L. Trimm, *J. Chem. Soc. Faraday Trans.* **1972**, *68*, 1406.
- [17] R. Burch, F. J. Urbano, P. K. Loader, *Appl. Catal. A* **1995**, *123*, 173–184.
- [18] D. Roth, P. Gélín, M. Primet, E. Tena, *Appl. Catal. A* **2000**, *203*, 37–45.
- [19] P. Castellazzi, G. Groppi, P. Forzatti, A. Baylet, *Catal. Today* **2010**, *155*, 18–26.
- [20] M. Berg, S. Järås, *Appl. Catal. A* **1994**, *114*, 227–241.
- [21] V. R. Choudhary, B. S. Uphade, S. G. Pataskar, *Appl. Catal. A* **2002**, *227*, 29–41.
- [22] C. F. Cullis, B. M. Willatt, *J. Catal.* **1983**, *83*, 267–285.
- [23] D. Roth, P. Gelin, A. Kaddouri, E. Garbowski, M. Primet, E. Tena, *Catal. Today* **2006**, *112*, 134–138.
- [24] A. V. Naumkin, A. Kraut-Vass, S. W. Gaarenstroom, C. J. Powell in *NIST Standard Reference Database 20, Version 4.1*, **2012**.
- [25] A. Tompos, J. L. Margitfalvi, M. Hegedus, A. Szegedi, J. L. G. Fierro, S. Rojas, *Comb. Chem. High Throughput Screening* **2007**, *10*, 71–82.
- [26] O. Balmes, A. Resta, D. Wermeille, R. Felici, M. E. Messing, K. Depert, Z. Liu, M. E. Grass, H. Bluhm, R. van Rijn, J. W. M. Frenken, R. Westerstrom, S. Blomberg, J. Gustafson, J. N. Andersen, E. Lundgren, *Phys. Chem. Chem. Phys.* **2012**, *14*, 4796–4801.
- [27] R. Bouwman, P. Biloen, *J. Catal.* **1977**, *48*, 209–216.
- [28] H. Karhu, A. Kalantar, I. J. Väyrynen, T. Salmi, D. Y. Murzin, *Appl. Catal. A* **2003**, *247*, 283–294.
- [29] D. Ciuparu, N. Katsikis, L. Pfefferle, *Appl. Catal. A* **2001**, *216*, 209–215.
- [30] D. Ciuparu, M. R. Lyubovsky, E. Altman, L. D. Pfefferle, A. Datye, *Catal. Rev.* **2002**, *44*, 593–649.
- [31] F. A. Marks, I. Lindau, R. Browning, *J. Vac. Sci. Technol. A* **1990**, *8*, 3437–3442.
- [32] Y. Zhang, G. Gajjala, T. Hofmann, L. Weinhardt, M. Bar, C. Heske, M. Seelmann-Eggebert, P. Meisen, *J. Appl. Phys.* **2010**, *108*, 093702–093706.
- [33] C. Hinnen, D. Imbert, J. M. Siffre, P. Marcus, *Appl. Surf. Sci.* **1994**, *78*, 219–231.
- [34] B. S. Ahn, S. G. Jeon, H. Lee, K. Y. Park, Y. G. Shul, *Appl. Catal. A* **2000**, *193*, 87–93.
- [35] V. Johánek, I. Stará, N. Tsud, K. Veltruská, V. Matolín, *Appl. Surf. Sci.* **2000**, *162–163*, 679–684.
- [36] A. Sarkany, *Appl. Catal. A* **1998**, *175*, 245–253.

Received: September 1, 2013

Revised: November 20, 2013

Published online on March 5, 2014